



Tricyclic imidazole antagonists of the Neuropeptide S Receptor

B. Wesley Trotter^{a,*}, Kausik K. Nanda^b, Peter J. Manley^b, Victor N. Uebele^c, Cindra L. Condra^c, Anthony L. Gotter^c, Karsten Menzel^d, Martin Henault^e, Rino Stocco^e, John J. Renger^c, George D. Hartman^b, Mark T. Bilodeau^b

^a Department of Medicinal Chemistry, Merck Research Laboratories, Boston, MA, USA

^b Department of Medicinal Chemistry, Merck Research Laboratories, West Point, PA, USA

^c Department of Neuroscience, Merck Research Laboratories, West Point, PA, USA

^d Department of Drug Metabolism, Merck Research Laboratories, West Point, PA, USA

^e In Vitro Sciences Group, Merck Canada, Montreal, Canada

ARTICLE INFO

Article history:

Received 8 March 2010

Revised 5 April 2010

Accepted 7 April 2010

Available online 13 April 2010

Keyword:

Neuropeptide S Receptor

ABSTRACT

A new structural class of potent antagonists of the Neuropeptide S Receptor (NPSR) is reported. High-throughput screening identified a tricyclic imidazole antagonist of NPSR, and medicinal chemistry optimization of this structure was undertaken to improve potency against the receptor as well as CNS penetration. Detailed herein are synthetic and medicinal chemistry studies that led to the identification of antagonists **1** and **NPSR-P11**, which demonstrate potent in vitro NPSR antagonism and central exposure in vivo.

© 2010 Elsevier Ltd. All rights reserved.

The neurotransmitter Neuropeptide S (NPS) was first reported in 2004 as a novel mediator of arousal and fear responses.¹ It was shown to activate the orphan G-protein coupled receptor GPR154, subsequently termed the Neuropeptide S Receptor (NPSR). While NPSR is expressed throughout the central nervous system, NPS precursor mRNA expression has been shown to be localized to a few specific regions of the brain.² Central administration of NPS has been shown to induce arousal and suppress sleep.¹ Thus, there has been interest in identifying small molecule antagonists of NPSR, and reports of two distinct classes of NPSR antagonists have recently appeared.^{3–5}

Here, we report a new class of potent NPSR antagonists identified at Merck and detail optimization efforts to improve potency and CNS penetration in this series. Racemic imidazole **1** (Fig. 1), identified in a high-throughput screening campaign, was a moderately potent NPSR antagonist (NPSR IC₅₀ 380 nM).⁶ Resolution of **1** gave potent enantiomer **2** (FLIPR IC₅₀ 163 nM).⁷

In vitro assays demonstrated that **2** was not a substrate of the human or rat PGP transporter and thus held promise as a starting point for optimized CNS-penetrant antagonists.⁸ While the compound exhibited a measurable free fraction in rat plasma (1%), it displayed poor membrane permeability (P_{app} 10×10^{-6} cm/s). In addition, broad counterscreening against a panel of unrelated enzymes and receptors indicated that **2** possessed a number of significant off-target activities that might confound interpretation of

behavioral effects in preclinical models.⁹ Given the lipophilic nature of **2** (measured log $P > 3.8$) we focused our efforts on increasing both polarity and potency in order to modulate physical properties and identify inhibitors with increased likelihood of specific, central NPSR antagonism in vivo.

The tricyclic core structure could be readily assembled from simple phenylimidazolines using a known lithiation/acylation/dehydration sequence.¹⁰ In a representative example (Scheme 1), phenylimidazoline **3** was treated with *n*-butyllithium and methyl-4-bromobenzoate to give adduct **4**. Heating this compound in acetic acid resulted in elimination of water (possibly via the intermediacy of an iminium 1,3-hydride shift)¹¹ to provide **5**. Deprotonation of the benzylic position of **5** has been reported in the literature to proceed via addition of NaH and to result in air oxidation of this scaffold. We found that alkylation of the sodium anion of **5** with

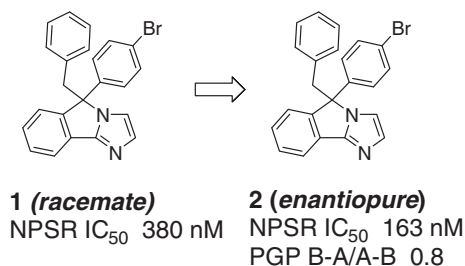
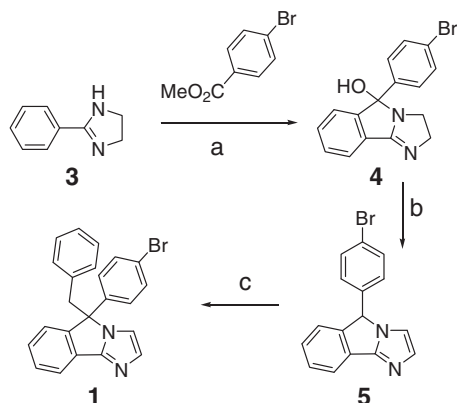


Figure 1. Tricyclic imidazole screening leads **1** and **2**.

* Corresponding author.

E-mail address: bwesley_trotter@merck.com (B.W. Trotter).

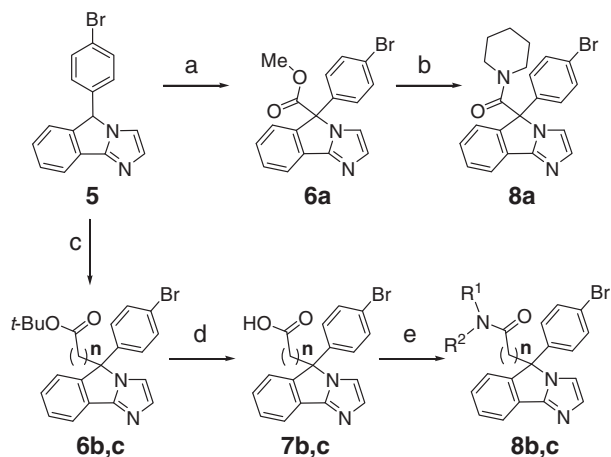


Scheme 1. Reagents and conditions: (a) *n*-butyllithium, 50 °C, 3 h, then methyl-4-bromobenzoate, rt, overnight, 55%; (b) AcOH, 125 °C, 5 h, 98%; (c) LDA, THF, -78 °C, then benzyl bromide, -78 to -30 °C, 92%.

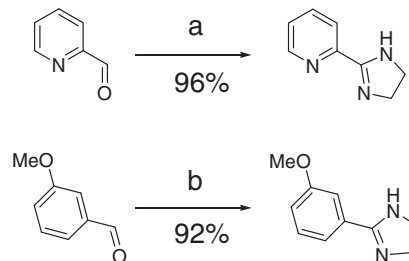
benzyl bromide to provide **1** was competitive with oxidation and proceeded in moderate yield. The yield of the alkylation process could be increased and the reaction extended to a wider variety of electrophiles by using LDA as the base at low temperature. This modification allowed replacement of the benzyl moiety with saturated alkyl groups as well as amide-containing electrophiles; electrophiles from both of these classes proved useful in modifying physical properties in this series.

Replacement of the benzyl group with amides and chain-extended amide substituents was also readily accomplished via the corresponding esters. As shown in Scheme 2, deprotonation of **5** with LDA followed by treatment with Mander reagent, *tert*-butylbromoacetate, or *tert*-butylbromopropionate provided esters **6a–c**. Compound **6a** was converted directly to the piperidine amide **8a** via trimethylaluminum-mediated transamidation. Compounds **6b** and **6c** were deprotected under acidic conditions to provide carboxylic acids **7b–c**. Amide coupling reactions provided compounds of type **8b–c**.

Variation of the fused aryl ring was most readily accomplished by synthesis of substituted arylimidazolines followed by recapitulation of the known lithiation/acylation/dehydration chemistry. Preparation of the requisite arylimidazolines is detailed in Scheme 3. This was generally accomplished via oxidation of



Scheme 2. Reagents and conditions: (a) LDA, THF, -78 °C, then methylcyanofornate, 67%; (b) piperidine, trimethylaluminum, toluene, 65%; (c) LDA, THF, -78 °C, then, for **6b** ($n = 1$), *tert*-butylbromoacetate, 81%; for **6c** ($n = 2$), *tert*-butylbromopropionate, 95%; (d) trifluoroacetic acid, CH₂Cl₂, quantitative; (e) HNR¹R², EDC, HOAt, *i*-Pr₂EtN.



Scheme 3. Reagents and conditions: (a) 1,2-ethylenediamine, I₂, K₂CO₃, *t*-BuOH, rt; (b) 1,2-ethylenediamine, NBS, CH₂Cl₂, 0 °C to rt.

in situ generated amins derived from the requisite aldehyde and 1,2-ethylenediamine.^{12,13}

Variation of the benzyl substituent was targeted initially as a synthetically viable approach to rapid modulation of physical properties (Table 1).¹⁴ Addition of polar substituents to the aryl ring met with limited success. While 2-CN analog **9a** preserved potency, no improvement in permeability or free fraction was evident. Evaluation of pyridine replacements identified 3-pyridyl variant **9b**, which displayed improved free fraction and permeability. We found that the use of saturated alkyl groups in place of the phenyl ring was tolerated (cyclohexane **9c** and cyclopentane **9d**). Incorporation of oxygen to provide tetrahydropyran **9e** resulted in improved potency versus NPSR as well as increased free fraction and permeability. A key limitation of **9e** was its rapid plasma

Table 1
Benzyl group SAR

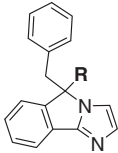
Entry	R	NPSR IC ₅₀ (nM) ^a	Plasma free fraction (%) ^b	PGP B–A/ A–B ^c	<i>P</i> _{app} (10 ^{–6} cm/s) ^d
9a		369	<1	1.7	17
9b		351	2.1	2.1	31
9c		254			
9d		321			
9e		92	19	1.2	31
9f		154			

^a Values represent the numerical average of at least two experiments. Interassay variability was $\pm 30\%$.

^b Measured via ultracentrifugation following incubation with rat serum.

^c Rat MDR1 directional transport ratio (B–A)/(A–B). Values represent the average of three experiments and interassay variability was $\pm 20\%$.

^d Passive permeability.

Table 2
Aryl group SAR


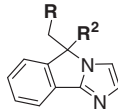
Entry	R	NPSR IC ₅₀ (nM) ^a
10a		336
10b		358
10c		1325
10d		387
10e		1725
10f		3166
10g		1500
10h		2179

^a Values represent the numerical average of at least two experiments. Interassay variability was $\pm 30\%$.

clearance in rat (Cl 48 mL/min/kg), which was expected to impede achievement of adequate CNS exposure in vivo.

A parallel investigation surveyed variants of the 4-bromophenyl substituent. Replacement of the bromo group with a number of heterocycles abrogated potency, indicating that there was little room for additional functionality at this position. However, replacement of the bromine with smaller substituents was less deleterious (**10a–10c**), and cyano analog **10d** preserved potency while significantly improving plasma free fraction and permeability (rat free fraction 17%, B–A/A–B 0.9, P_{app} 33×10^{-6} cm/s). 3-Bromophenyl antagonist **10e** displayed reduced potency as did the corresponding 3-CN analog **10f**. Bromopyridine analogs **10g** and **10h** were also significantly less potent than lead **2**.

Straightforward additivity was not observed upon combining modifications of the benzyl and phenyl substituents (Table 3). Combinations of the methylene-linked THP group found in **9e** with tolerated phenyl groups such as 4-cyanophenyl (**11a**) and 4-fluorophenyl (**11b**) resulted in significant losses in potency. 4-Chlorophenyl analog **11c** proved to be one of few suitable combinations, with good NPSR potency and higher free fraction and permeability than **2**. A broadened survey of substituent combinations provided some unexpected results, including cyanophenyl cyclopentyl antagonist **11e**. This antagonist was among the most potent combinations despite no evident potency benefit from either of these groups individually (**9d**, Table 1, and **10d**, Table 2). Free fraction in the range of 1–2%, lack of PGP susceptibility, and good permeability were generally observed in this group of saturated analogs (Table 3), but no significant improvements in rat pharmacokinetic properties were realized.

Table 3
Substituent combinations


Entry	R ¹	R ²	NPSR IC ₅₀ (nM) ^a	Plasma free fraction (%) ^b	PGP B–A/A–B ^c	P_{app} (10^{-6} cm/s) ^d
11a			635			
11b			660			
11c			134	1.8	1.4	31
11d			851	1.3	1.3	25
11e			145	1.1	0.6	22
11f			114		1.6	17

^a Values represent the numerical average of at least two experiments. Interassay variability was $\pm 30\%$.

^b Measured via ultracentrifugation following incubation with rat serum.

^c Rat MDR1 directional transport ratio (B–A)/(A–B). Values represent the average of three experiments and interassay variability was $\pm 20\%$.

^d Passive permeability.

In order to further modulate physical and pharmacokinetic properties, incorporation of amide functionality into the alkyl substituent connective framework was investigated (Figure 2). While the initially targeted analog **8a** resulted in a significant loss of potency, synthesis of a series of methylene-linked amides revealed a strong dependence of potency on the length of the linker region. Propionamide **13** was >10-fold more potent than **8a**. Importantly, chain-extended amides **12** and **13** were not substrates of the PGP transporter (Figure 2).

Optimization of potency and physical properties in this amide series was pursued via a rapid analog approach. Simple amide coupling enabled a survey of piperidine replacements. Table 4¹⁵ shows representative results from a library based on the 4-chlorophenyl substituted scaffold. We observed that relatively small cyclic and acyclic dialkyl amides were potent NPSR antagonists. Plasma free fraction was found to vary inversely with susceptibility to PGP; thus a balance between these two factors had to be achieved. A leading example of this was that incorporation of a pyrrolidinylethyl substituent on the piperidine (**14c**) retained potency and

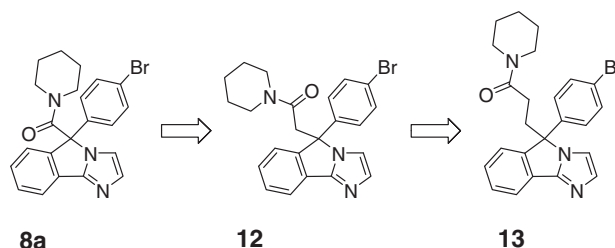
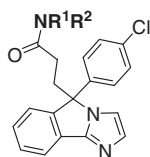
**Figure 2.** Amide antagonists.

Table 4
Amide optimization

Entry	NR¹R²	NPSR IC ₅₀ (nM) ^a	Plasma free fraction (%) ^b	PGP B–A/A–B ^c	Rat clearance (mL/min/kg) ^d
14a		131	1.1	1.6	20
14b		96	0.8	1.4	26
14c		126	8.1	34.2	38
14d		138	0.7	2.3	31
14e		95	0.6	1.7	34
14f		92	0.6	1.5	36
14g		90	2.2	2.1	38
14h		239	2.9	2.0	9

^a Values represent the numerical average of at least two experiments. Interassay variability was $\pm 30\%$.^b Measured via ultracentrifugation following incubation with rat serum.^c Rat MDR1 Directional Transport Ratio (B–A)/(A–B). Values represent the average of three experiments and interassay variability was $\pm 20\%$.^d IV clearance measured in cassette dosing experiments. Clearance for **14g** is quoted for the racemic form.

substantially increased free fraction but also transformed the compound into a PGP substrate. Modulation of amine basicity via fluorination resulted in PGP non-substrate **14h**. While generally improved relative to precursor compounds, plasma clearance in this series was significantly dependent on the identity of the amide group. The simple diethyl amide **14g**¹⁶ balanced these factors well, combining $>2\%$ free fraction with low PGP susceptibility and moderate clearance. However, **14g** exhibited low exposure when dosed orally to rats ($AUC_{0-\infty}$ 0.18 $\mu\text{M}\cdot\text{h}$ at 10 mg/kg).

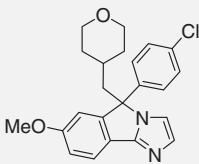
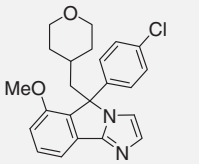
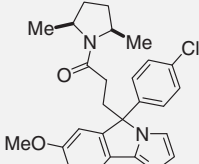
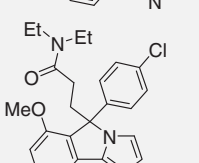
Having identified both the THP-methyl and diethylamino-propionate subunits as motifs with free fraction and PGP properties suitable for CNS penetration, we attempted to further improve potency and oral exposure via tuning of substitution on the tricyclic core. Among substituents surveyed on the fused benzo ring,¹⁷ few were tolerated, and the methoxy group was unique in its improvement of potency versus NPSR. Both the amide and THP-containing antagonists gained potency via methoxy substitution at both the 6- and 7-positions. Compounds **15** and **NPSR-P11**¹⁸ were identified as particularly potent THP and amide antagonists with $>1\%$ plasma free fraction and minimal PGP transport.¹⁹ Both compounds were counterscreened against broad panels of enzymes, receptors and ion channels and found to exhibit much improved profiles relative to lead **2**.²⁰

Plasma exposure of each compound when dosed orally to rats was relatively low (Table 5), but we found that good peripheral and central exposure could be achieved by IP dosing. **15** achieved cerebrospinal fluid (CSF) levels (representative of unbound compound levels in the brain)²¹ of 594 nM (30 min) and 153 nM (2 h) when dosed at 75 mpk to rats as a solution in 25% HPB-cyclodextrin. CSF/plasma ratios of 1% were observed at each time point and corresponded to the observed plasma free fraction. Thus the compound exhibited CNS exposure well above its IC₅₀ for NPSR antagonism.

NPSR-P11 was dosed at 30 mpk IP to rats. Plasma levels measured at 30 min, 1 h, and 2 h were 7.8 μM , 5.1 μM , and 3.0 μM , respectively. These concentrations correspond to unbound exposures of 101 nM, 66 nM, and 39 nM, at or above the NPSR IC₅₀. The exposures observed for both **15** and **NPSR-P11** relative to IC₅₀ are comparable to exposures demonstrated to result in NPSR receptor occupancy in vivo in a separately reported antagonist series.³

In summary, a new structural class of NPSR antagonists has been identified. Optimization provided compounds that were not substrates of rat PGP and exhibited significant plasma free fractions, enabling in vivo CNS exposure upon IP dosing. This new class of NPSR antagonists provides additional tools for in vivo studies of the relevance of NPSR to behavioral modification.

Table 5
Optimal core substituents

Entry	Structure	NPSR IC ₅₀ (nM) ^a	Plasma free fraction ^b	PGP B–A/A–B ^c	Rat AUC (PO, dose) ^d
15		82	1.6	1.3	0.114 μM-h (2 mpk)
16		46	0.8	na	0.425 μM-h (10 mpk)
17		50	0.7	2.2	0.115 μM-h (2 mpk)
NPSR-PI1		43	1.3	2.9	1.15 μM-h (10 mpk)

^a Values represent the numerical average of at least two experiments. Interassay variability was ±30%.

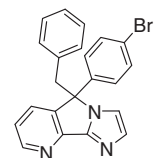
^b Measured via ultracentrifugation following incubation with rat serum.

^c Rat MDR1 Directional Transport Ratio (B–A)/(A–B). Values represent the average of three experiments and interassay variability was ±20%.

^d Dosing vehicle: 20% aqueous Vitamin E/TPGS.

References and notes

- Xu, Y. L.; Reinscheid, R. K.; Huitron-Resendiz, S.; Clark, S. D.; Wang, Z. W.; Lin, S. H.; Brucher, F. A.; Zeng, J. A.; Ly, N. K.; Henriksen, S. J.; Lecea, L. C.; Civelli, O. *Neuron* **2004**, *43*, 487.
- Xu, Y. L.; Gall, C. M.; Jackson, V. R.; Civelli, O.; Reinscheid, R. K. *J. Comp. Neurol.* **2007**, *500*, 84.
- Melamed, J. Y. et al *Bioorg. Med. Chem. Lett.* **2010**, *20*, 4700.
- Okamura, N.; Habay, S. A.; Zeng, J.; Chamberlin, A. R.; Reinscheid, R. K. *J. Pharmacol. Exp. Ther.* **2008**, *325*, 893.
- Zhang, Y.; Gilmour, B. P.; Navarro, H. A.; Runyon, S. P. *Bioorg. Med. Chem. Lett.* **2008**, *18*, 4064.
- A dual sequence FLIPR (Fluorometric Imaging Plate Reader) Ca²⁺ mobilization assay was used to evaluate compounds for agonist and antagonist activity on the Neuropeptide 5 Receptor expressed on recombinant CHOK1 cells plated in 384 well PDL coated plates 24 h prior to experiment (15 K cells/well/20 μL). Following washing with buffer and loading with Fluo4AM dye for 1 h at 37 °C in 5% CO₂, cell plates were placed in the FLIPR and incubated with titrated compounds for 4 min during sequence 1 data collection. In sequence 2, an EC₈₀ of human NPS was added to the assay plates and data collected for another 4 min. Percent stimulatory activity (sequence 1) or inhibition (sequence 2) was calculated relative to Ca²⁺ mobilization in NPS stimulated control wells (EC₁₀₀ or EC₈₀ NPS). Compound potencies were determined from plots of concentration response curves using 4p logistical fits and reported as means ± S.D. of multiple determinations.
- ent-**2** was significantly less potent (NPSR IC₅₀ 1987 nM).
- Miller, D. S.; Bauer, B.; Hartz, A. M. *S. Pharmacol. Rev.* **2008**, *60*, 196.
- IC₅₀ values ranging from 1 to 8 μM were reported for several GPCRs, ion channels, and enzymes with potential CNS relevance (MDS Pharma Services).
- Houlihan, W. J.; Parrino, V. A. *J. Heterocycl. Chem.* **1981**, *18*, 1549.
- Cook, A. G.; Switek, K. A.; Cutler, K. A.; Witt, A. N. *Lett. Org. Chem.* **2004**, *1*, 1.
- Fujioka, H.; Murai, K.; Ohba, Y.; Hiramatsu, A.; Kita, Y. *Tetrahedron Lett.* **2005**, *46*, 2197.
- Ishihara, M.; Togo, H. *Tetrahedron* **2007**, *63*, 1474.
- Except where noted, compounds were synthesized and tested in racemic form.
- Except where noted, compounds were synthesized from racemic acids of type 7. Stereogenic amines were also introduced as racemates to afford diastereomeric mixtures; in order to accelerate screening, diastereomers were not separated.
- Single enantiomer, obtained from the enantiopure carboxylic acid precursor, which was separated via chiral HPLC (analytical: SFC-OD-H column (4.6 × 250 mm), MeOH/CO₂ (20:80, 4 mL/min), retention time 5.7 min (slower eluting peak). Absolute stereochemistry has not been determined.
- Methyl substitution was tolerated but did not improve physical properties. Cyano groups as well as larger alkoxy substituents led to loss of NPSR antagonist potency. Pyridinyl replacements for the fused benzo ring also resulted in potency decreases. Benzyl variant **i** (NPSR IC₅₀ 1458 nM) is a typical example.



- Single enantiomer, obtained via chiral HPLC (SFC-AD-H column (2 × 25 cm), EtOH/CO₂ (15:85, 70 mL/min), retention time 5.2 min (faster eluting peak). Absolute stereochemistry has not been determined.
- An HPLC log D of 3.2 was measured for **15**.
- Against a panel of 163 enzymes, receptors and ion channels, **15** showed IC₅₀ values <10 μM in only four assays: thromboxane A2, 7 μM, melatonin, 1.3 μM, rabbit monoamine transporter, 7 μM, and sodium channel site 2, 4 μM. Against a panel of 36 CNS-relevant enzymes and receptors, **NPSR-PI1** showed an IC₅₀ value <10 μM in only one assay: CB1 receptor, 6 μM.
- Liu, X. R.; Smith, B. J.; Chen, C.; Callegari, E.; Becker, S. L.; Chen, X.; Cianfrogna, J.; Doran, A. C.; Doran, S. D.; Gibbs, J. P.; Hosea, N.; Liu, J. H.; Nelson, F. R.; Szewc, M. A.; Van Deusen, J. *Drug Metab. Dispos.* **2006**, *34*, 1443.